SEMARAK ILMU PUBLISHING

Journal of Advanced Research in Applied Sciences and Engineering Technology

https://semarakilmu.com.my/journals/index.php/applied_sciences_eng_tech/index
ISSN: 2462-1943

Implementation of Two-Stage Multilevel Inverter System Using PIC Controller

M. Saifizi[1,*], M. I. Fahmi[1], M. Othman[1], Wan Azani Mustafa[1], M. Z. Aihsan[1], M. R. Manan[1], Azri A. Aziz[1]

[1] Faculty of Electrical Engineering Technology, Universiti Malaysia Perlis, Pauh Putra Campus, 02600 Arau, Perlis, Malaysia

ABSTRACT

In this study, the Cascaded H-Bridge Multilevel Inverter (CMLI) is described for use with infrared dryer loads. Because of the low harmonic distortion content and reduced voltage stress in the switching devices, CMLI is one of particular interest. The CMLI topology and the Selective Harmonic Elimination Pulsed Width Modulation (SHEPWM) technology were studied and evaluated. To evaluate the inverter, SHEPWM modulation was studied and applied. The system also includes a DC-DC converter. The converter was designed to be used in infrared drying system powered by direct current (DC) power where an increased output voltage is required. This study also presented an evaluation of performance using infrared load of the CMLI based on power used at 100 W. As a result, a comparison of input power was made, and an assessment into the converter's power quality in terms of harmonic content and overall efficiency was conducted. The implementation of the system by hardware had been able to reduce the harmonic to 15.5%.

Keywords:
Two-stage inverter; multilevel inverter; boost converter; Cascaded H-bridge; DC-DC converter

Received: 28 August 2022 **Revised: 3 October 2022** **Accepted: 4 October 2022** **Published: 17 October 2022**

1. Introduction

Single-stage inverters and two-stage inverters are the two types of grid-connected PV inverters. Each PV module connected in series to the inverter was connected to the inverter through a string in this single-stage string inverter configuration [1]. These inverters harvested more energy than centralized inverters and were also easier to configure [1,2]. However, to achieve a higher output voltage in regular operation, many PV modules had to be connected in series [1]. This increased the overall cost of the configuration.

A DC/DC converter integrates the PV panel with the DC/AC inverter. Usually, this configuration is applied in two-stage inverters design. Subsequently, a DC/DC boost converter must be linked together with a low output voltage PV panel. Then the enhanced output voltage is transformed into AC voltage source [3]. Line-frequency transformers have been used largely to link solar systems to the grid in order to establish galvanic isolation in grid-connected photovoltaic

* *Corresponding author.*
E-mail address: saifizi@unimap.edu.my

https://doi.org/10.37934/araset.28.2.4155

inverters. The installation of these transformers was challenging due to their size and weight. They were also inefficient and added to system complexity due to multiple power levels [4].

Transformerless inverters were developed to address inverter efficiency, cost, and size issues. When the transformer is removed, the photovoltaic system and the power grid form a galvanic connection. As a result, the parasitic capacitors allow common-mode leakage current to flow between the photovoltaic system and the ground [5].

In addition to increasing system losses and grid current harmonics, this leakage current also pricipitate a major safety danger [6]. Therefore, the common-mode leakage current must be taken into account while developing a transformerless PV inverters.

The amount of solar emission and the surrounding temperature have a direct correlation with a PV system's performance. When it comes to power applications, a PV system's efficiency must be high if it is to feed power into the grid. As a result, monitoring the maximum power output under various environmental conditions is necessary. The first stage of a two-stage inverter that is known as DC/DC boost converter, controls the DC-link voltage and supplies the second stage with the most power possible in order to increase the effiency [7,8]. The maximum power generated in the first stage is being mapped using a variety of controllers, including P&O, fuzzy, neural network, sliding mode controller, and others [9]. The control system assures power quality and balance are maintained in the second stage. Since the conversion process depends on the control algorithms, proper inverter controllers are required in PV applications to increase inverter effectiveness [10].

Predominantly in PV and other electronic control systems, it can be state that output voltage can be modified by utilizing the DC/DC power converters. In addition, to monitor the amount of power produced from the PV panel, a DC/DC converter is often equipped between the load and the panel. This is helpful for a PV system with irregular and intermittent output. If the PV system includes the combination of AC and DC converters, a DC-link capacitor can enhance the constancy of the DC output voltage and minimise the impact of variations on the AC output [10]. CUK converters and step-boost converters are examples of DC-converters that can boost (step-up converters), buck (step-down converters), or combine the two. The converter type can be selected depending on the required output voltage capacity or magnitude in order to supply the correct voltage source to the inverter with dc rectification and control potentialities [11]. This is advantageous for stand-alone, grid-connected, and hybrid power systems respectively. These solutions enable the PV system to produce more power since the DC/DC converter has an optimum power operating algorithm. An inverter's power output tends to differs with subject to the application complied.

A power electronic converter that converts DC to AC is known as an inverter to produce a sinusoidal alternating current (AC) with adjustable frequency and magnitude [12,13]. A constant voltage is fed to a voltage source inverter (VSI), while a constant current is fed to a current source inverter (CSI). In most cases, VSIs are used in applications that require powerful AC motor drives.

The power stage of the single-phase inverter consists of two branches, a DC-input voltage source and a DC-link capacitor (VDC). A stabilized voltage source that may be utilized with the DC -Link capacitor is the DC -input voltage source. The inverter's parameters will manipulate the magnitude of the DC input voltage. Moreover, a single-phase inverter's should obtain the higher amplitude of input DC voltage than the inverter's maximum AC output voltage in a power system. Referring to PV panel case, concerning that the DC-link voltage is steady while switching between power devices, the capacitor's properties are significant when the input power DC varies [14]. To generate the optimized output power, the DC -link capacitance must be adequate to decrease the DC -link voltage fluctuation [15]. The DC/AC conversion procedure involves switching devices as a key factor. To prevent the branches from ever running at the same time, two insulated gate bipolar transistors (IGBTs) with antiparallel diodes are employed in each branch [16]. The switching device

chosen is determined by the system's specific design, such as switching speed and power capacitance. MOSFETs are typically used to provide low power capacitance with fast switching speeds, whereas IGBTs are typically used to provide higher power capacitance with medium switching speeds [2]. A multilevel inverter system that operates efficiently in boost mode is discussed. The multilevel inverter's mode is defined by the boost converter's output voltage, which is controlled by a control algorithm.

This study proposes a transformerless multilevel inverter to simulate and develop for infrared dryer application. The multilevel inverter is designed based on a microcontroller seven-level single-phase inverter. The seven-level inverter is controlled with Selective Harmonic Elimination Pulse Width Modulation (SHEPWM). This approach eliminates selected low order harmonics, which third, fifth and seventh order harmonic elimination as a comparison. The output power of the multilevel inverter is also designed to produce low AC power below 1000 watts. In conclusion, the inverter configurations consisted of two-stage inverters: integration DC boost converter and multilevel inverter. The system's two-stage inverter contains a boost converter connected in series with each DC input power. It is used for DC-DC conversion and produces a regulated output voltage, which is then handled by the DC -AC inverter in the circuit. A Cascaded H-Bridge Multilevel Inverter (CMLI) is used, which is switched at the frequency of infrared light. This CMLI was used as the multilevel inverter.

2. Methodology

The stepped voltage for a 7-level inverter is commonly calculated using the SHE technique. There are three positive steps (V_{dc}, $2V_{dc}$, $3V_{dc}$) during the positive half-cycle of the inverter output waveform. For a seven-level inverter, the Fourier expression of the inverter output voltage for SHE modulation is:

$$V_{inv}(\omega t) = \frac{4V_{dc}}{n\pi}\sum_{n=1.3,5}^{\infty}[cos(n\theta_1) + cos(n\theta_2) + cos(n\theta_3)]sin(n\omega t) \quad (1)$$

where ϑ_1 ~ ϑ_3 are the switching angles in the first quarter waveform at each level, and they must satisfy the following condition: $\vartheta_1<\vartheta_2<\vartheta_3<\pi/2$. The following equations can be used to calculate the switching angles:

$$\begin{aligned} cos(\theta_1) + cos(\theta_2) + cos(\theta_3) &= \frac{\pi V_1}{4sV_{dc}} \\ cos(3\theta 1) + cos(3\theta_2) + cos(3\theta_3) &= 0 \\ cos(5\theta_1) + cos(5\theta_2) + cos(5\theta_3) &= 0 \end{aligned} \quad (2)$$

The relationship of the fundamental voltage V_f with modulation index M can be formulated by:

$$M = \frac{\pi V_f}{4sV_{dc}}, 0 \leq M \leq 1 \quad (3)$$

In a quarter waveform, s represented the number of positive steps. This results in the required fundamental voltage, allowing the most significant low-order harmonic components to be eliminate. Figure 1 illustrates a 7-level symmetrical CMLI inverter arrangement constitutes of three H-bridge

cells. Each of H-bridge cell constituted of four power switches and a single dc voltage source that was connected to the cell through a dc link capacitor.

The switching instants on the time axis are obtained by solving nonlinear transcendental algebraic iterative numerical equations such as the Newton Raphson process. By iteration in MATLAB, the switches angle for the seven-level H-Bridge Cascade multilevel inverter was calculated. Meanwhile, the switching sequence for the multilevel inverter is configured by using microcontroller.

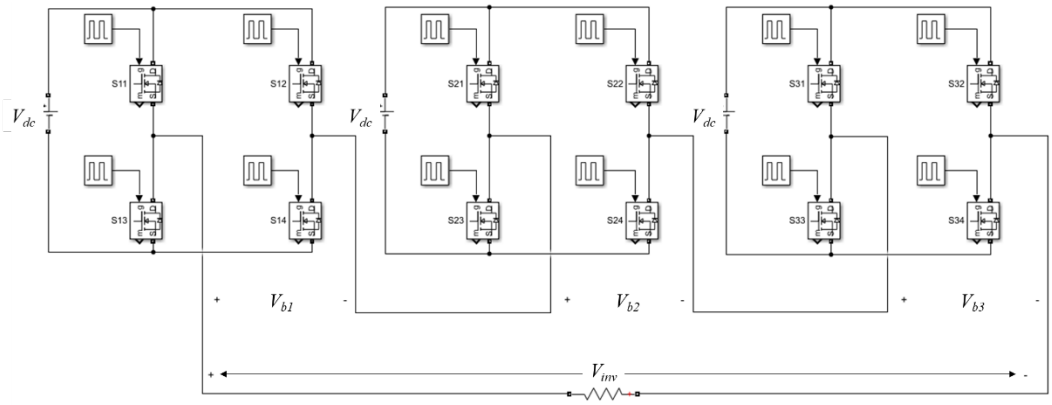

Fig. 1. Configuration of 7-level inverter system

An experimental study will be conducted to validate simulation data with real-time performance. This experiment uses the same method and the same parameters as the simulation except for output voltage. As shown in Figure 2, this multilevel inverter system consists of integration with 1-unit PIC microcontroller, 3 units DC converter, 12-units gate driver, 3-units full H-bridge and 1-unit infrared load.

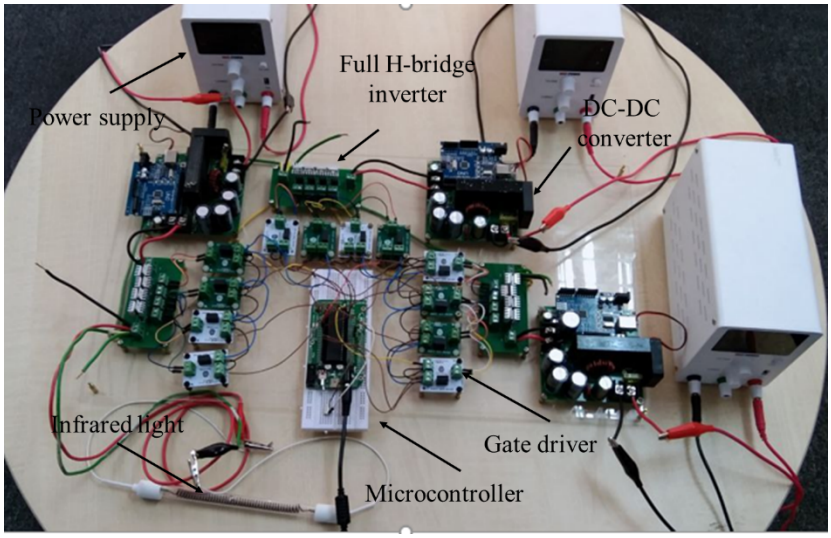

Fig. 2. Two-stage multilevel inverter experimental setup

Meanwhile, details on the design and configuration of the boost converter are described as shown in Table 1.

Table 1
Parameter of developed DC-DC boost converter

Name	Symbol	Value
Diode	D, D1, D2	0.001 Ω
Resistance	R3	0.3 Ω
Inductance	L	100 µH
Intermediate capacitor	C, C1	100, 470 µF
Output capacitor	C3, C4, C5, C6	0.002, 0.1, 330, 330, 330 µF
Load resistance	R2	200 Ω

The Figure 3 and 4 show DC-DC boost converter system that used in this experiment. The converter is controlled by Arduino Uno to maintain 110 V.

Fig. 3. DC-DC boost converter system prototype

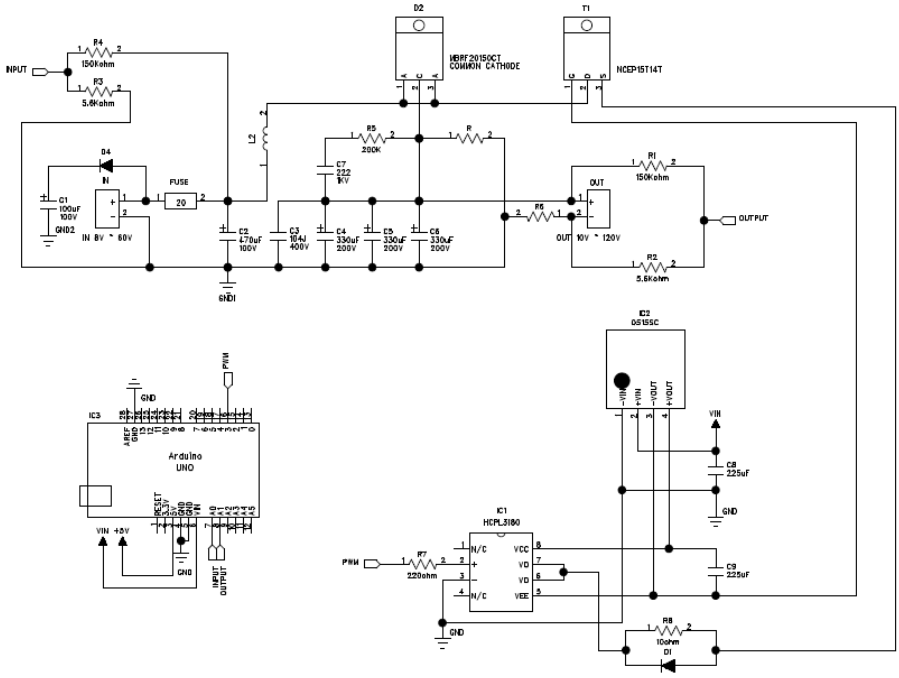

Fig. 4. DC-DC boost converter system schematic

The converter is programed using Simulink to read the voltage divider and control the PWM duty cycle of the MOSFET based on proportional controller as shown in Figure 5. The proportional controller is tuned up based on trial-error method, where is the K_p is set up as 10.

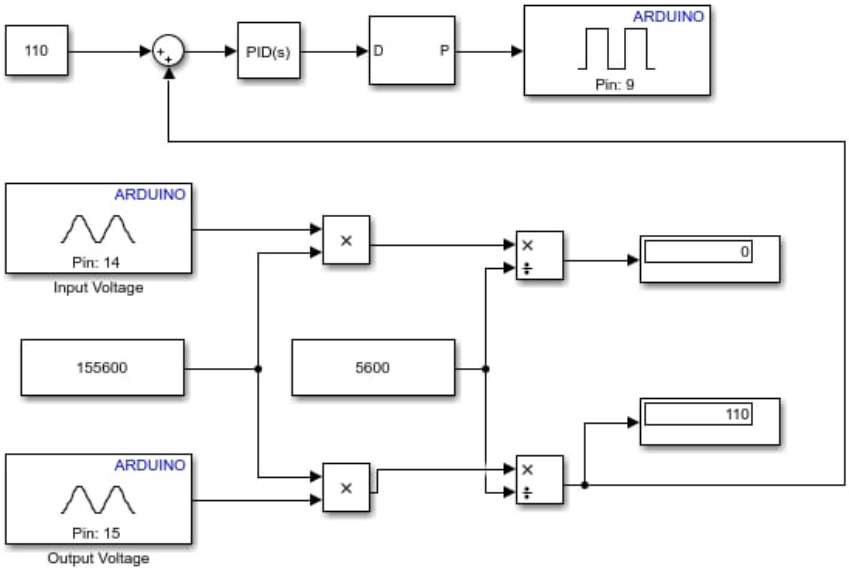

Fig. 5. Simulink programming for Arduino controller

The full H-bridge serves to connect the DC boost converter and Vout respectively as shown in Figure 6. Each full H-bridge circuit configures 4 MOSFETs at S1~S4 to determine the polarity of the output voltage. The gate drivers J1~J4 are applied to produce the appropriate high current gate drive for an input gate of MOSFET. The dc-dc boost converter was linked to the full H-bridge input to ensure that the voltage injected into the full H-bridge was sufficient to provide the needed inverter output.

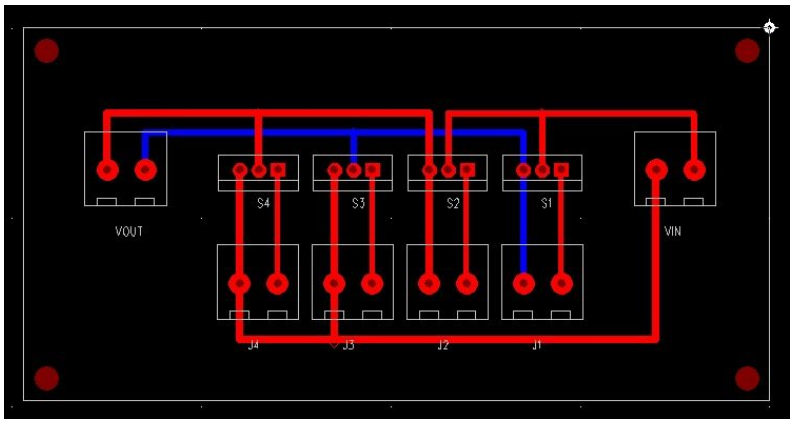

Fig. 6. Single phase full H-Bridge inverter configuration

The experiment was set up as shown in Figure 2, with PIC as the controller, to validate the simulation findings of 7-level inverter structures and control algorithm. The power switching devices of the single-phase CMLI prototype were 12 units IRF840 Mosfets with built-in quick recovery diodes. The inverter was loaded with 150 watts of infrared light. Using a Tektronix DP04054 Digital Phosphor Oscilloscope, the inverter output voltage waveform, each bridge output waveform, and output THD are measured and obtained. Meanwhile, input current of the Converter and output current of the inverter were measured using Teledyne LeCroy Oscilloscopes model Wavesurfer 3024.

Two voltage signals, V_{ref} and V_{act}, were injected to a comparator in a closed-loop boost converter system. The invalid frequency was injected to R-S flip flops, which generate the switch's pulse, together with the exact frequency. Our proposed system was supposed to maintain an output of 110 V when the input range is 18 V~24 V, making it convenient to be deployed for various industrial purposes.

The DC-DC converter had experimented with a variation of the input voltage. The output voltage was detected by voltage divider; it is then compared to a reference voltage. The PWM was adjusted to maintain the required output voltage by the defect elimination by a proportional controller, which is the proportional controller's output.

The experiment setup is conducted to measure the boost converter performance. This experiment is to analyse whether the converter is compatible with the input voltage for the inverter. In the interest of performance demonstration for this converter, a few current input and voltage output responses need to be observed.

As mentioned before, the simulation uses 220 V input to integrate with the infrared light as a load. Therefore, each converter circuit will produce around 110 V_{dc} for each multilevel input power source to generate 220 V_{rms}. Meanwhile, this practical experiment will apply the same method to eliminate the harmonic order in the output voltage, as demonstrated in the previous section.

This two-stage inverter module circuit is intended for DC-DC conversion and combined with a CMLI for DC-AC conversion. The input voltage for the entire framework is set at 18, and 24 V, which is the maximum power point voltage of a standard solar panel. The input power for a standalone PV configuration is approximately 100 W, which corresponds to the power rating of the solar panel. In this experiment, a regulated DC power supply is used, maintaining a constant output voltage regardless of the change in the AC output signal.

To assess the existence of undesirable components in a signal, certain metrics were used. THD (Total Harmonic Distortion) is one such statistic, which was consisted of the RMS values of the undesired and fundamental parts. A waveform's THD indicates how many undesired components are present in the signal. The larger the THD of a waveform, the more ununundesired components were present in the signal.

$$THD = 100 \times \sqrt{\frac{\sum_{n=2}^{\infty}(f_n)^2}{(f_1)^2}} \quad (4)$$

Based on the magnitude of the load and the size of the power system to which it is linked, the standard provided various distortion limitations. To calculate a system's THD, apply Equation 4 to the voltage waveform.

3. Results

The proposed inverter module has been tested for multi input configurations by using the multilevel inverter concept, thus, called modular multilevel inverter. The inverter module has been tested as a standalone system by connecting it to the load.

The modular multilevel inverter structure was tested for the PV inverter system as a standalone system for AC infrared load applications. In this scheme, for less wattage configuration, generally less than 1000W, the system is sufficient enough to run the AC infrared loads. In order to extract most of the power from the connected components, CMLI were designed taking into consideration all the design and energy harvesting parameters.

3.1 7-Level Symmetrical CMLI with 18V Input Voltage

The output of this system is shown in the Figure 7. This framework is then connected in series with other power inputs to evaluate the multilayer inverters' functionality. The values of power input have been varied to get the necessary output voltage levels. For a 7 level output voltage multilevel inverter, three power inputs are connected in series (n =3). The experimental findings of a 7-level CHB inverter linked to three H-bridge cells when tested with infrared light load. A 110 V_{dc} voltage is applied to each H-bridge cell, which is the supply was boosted up by converter form 18 V_{dc} power supply. The output voltage waveform of a 7-level CMLI was shown in Figure 7(a), and the output voltage THD was 15%. The 5^{th} and 7^{th} harmonics were eliminated, as seen in Figure 7(b).

Figure 7(a) shows that the total output voltage of multilevel inverter is the sum of the individual voltages found across each of the output bridge as shown in Figure 8(a), (b), (c). The Figure 7(c) of this plot shows the current values for this configuration and the RMS current is 0.77 A_{rms}. Therefore, the total power provide to the infrared load by CMLI system is 171 W.

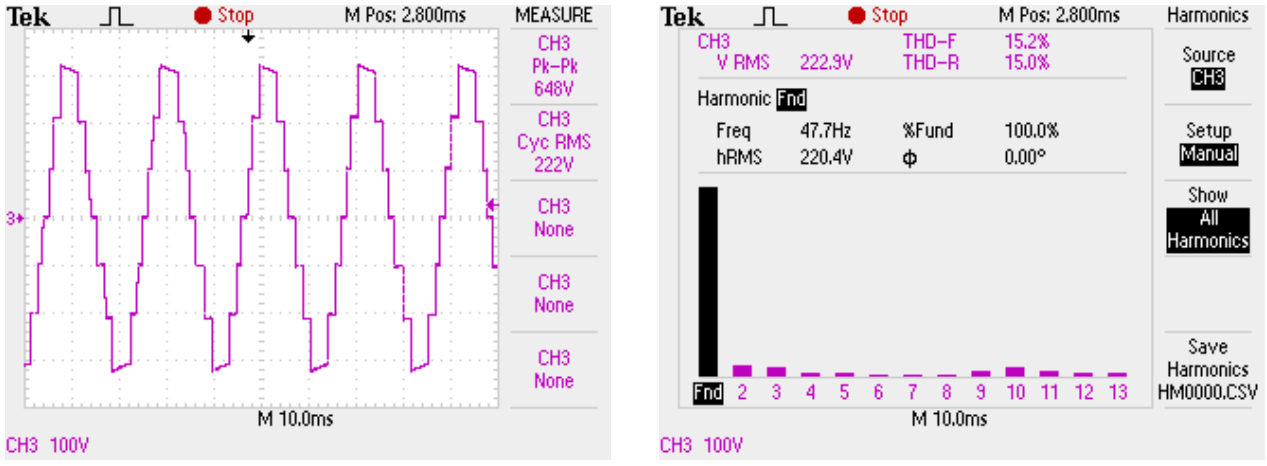

(a) (b)

(c)

Fig. 7. The 7-level symmetrical CMLI of (a) the output voltage waveform, (b) the output voltage THD, (c) the output current, when 18 V input voltage of converter is injected

The output voltage of the complete configuration is found to be reached the desired output voltage as shown in Figure 4.10 (a), (b), (c). This will increase the voltage and the power rating of each of the input configurations.

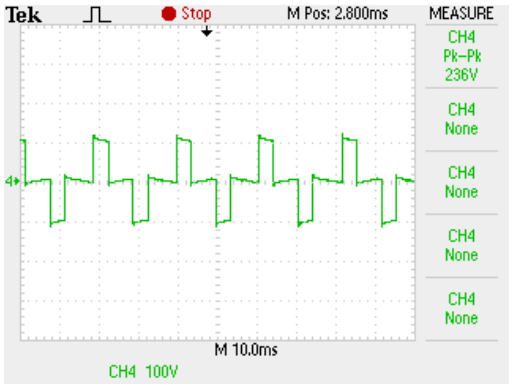

(a)

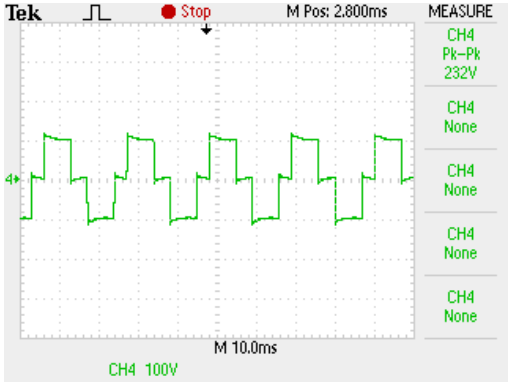

(b)

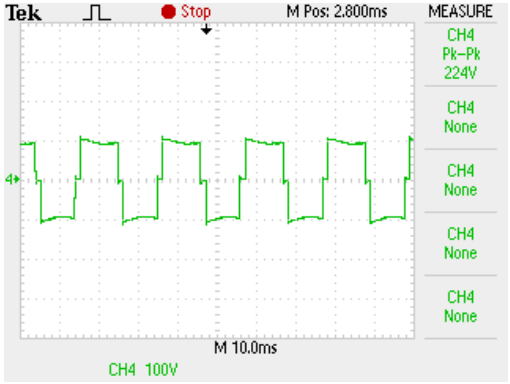

(c)

Fig. 8. Individual bridge voltage for 7 level CMLI when the input voltage converter is 18 V

The output voltage of the complete configuration is found to be reached the desired output voltage as shown in Figure 8(a), (b), (c). This will increase the voltage and the power rating of each of the input configurations.

As long as the reference voltage remains less than the input voltage, the complete system works in the boost mode. Here, we are considering the input voltage to be 18V. The boost converter's output voltage serves as the reference voltage. As a result, the system operates in boost mode anytime the voltage level was less than 110V.

The input voltage is supplied via the power supply unit. It is specified to 18 V, considering that the standard DC sources only supply the voltage to that specific level. The output converter is connected to the CMLI circuit to observe the current input consumption. The Figure 9 shows that all three converter consumed about 7~10 A to step up voltage from 18 V to 110 V.

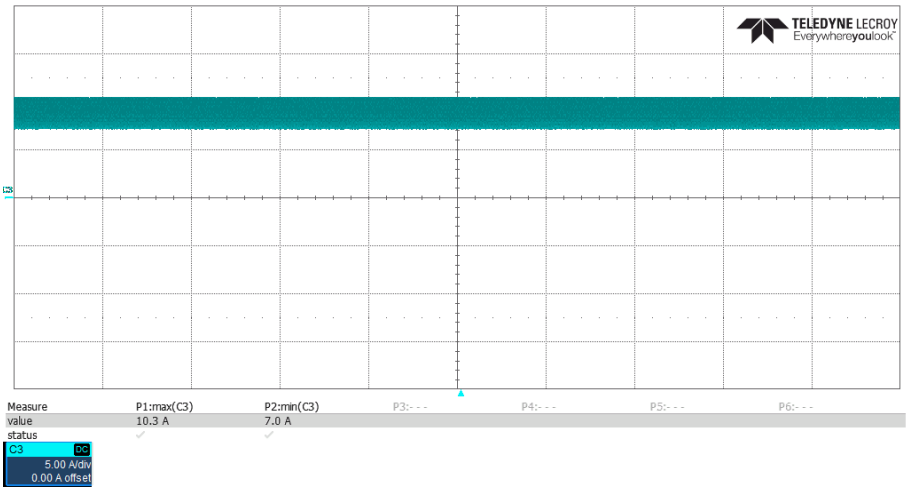

(a)

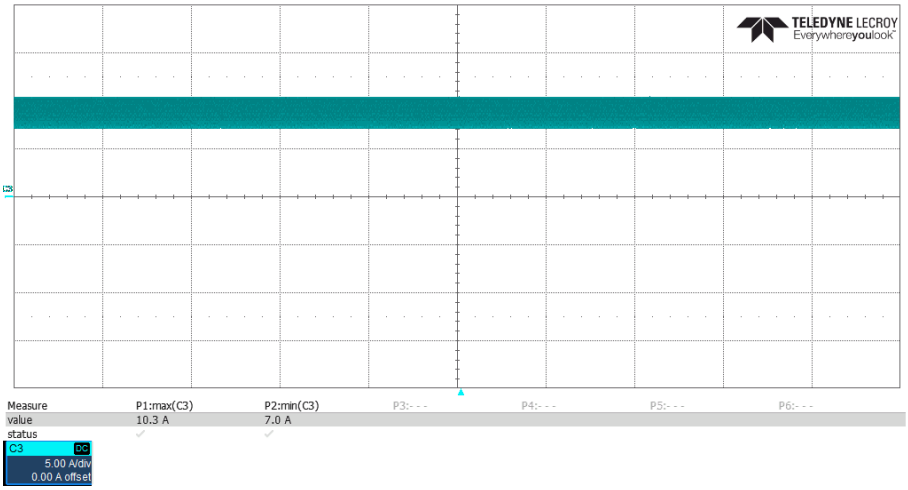

(b)

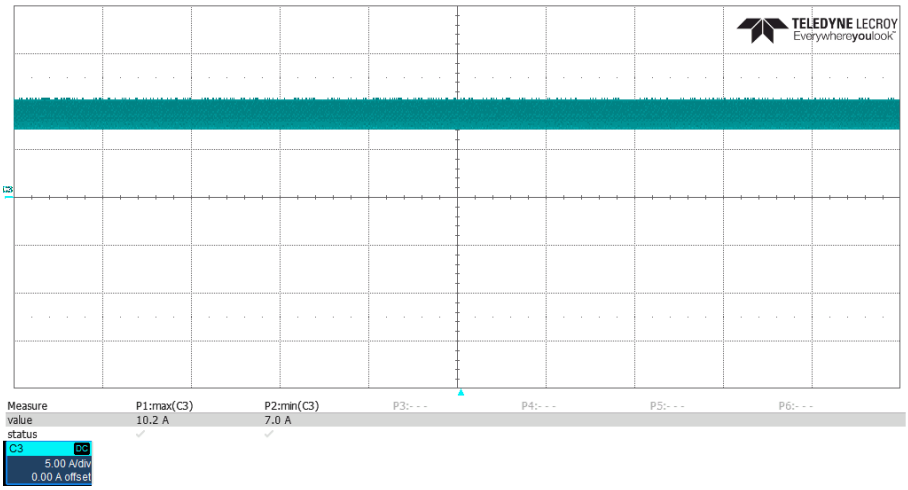

(c)

Fig. 9. Input current consumed of all three converters when step up voltage from 18 V to 110 V

3.2 7-Level Symmetrical CMLI with 24V Input Voltage

The input and output parameters characteristics are observed through the oscilloscope, as shown in the figures below. The configuration setup for this measured value is not the same as each other as the output voltage, output current and input current are set to different values per division.

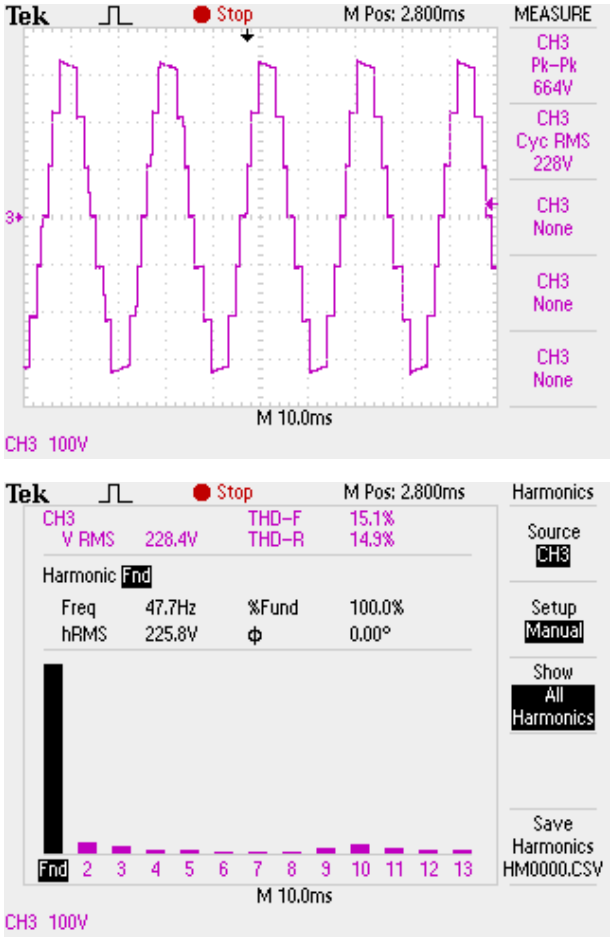

(b)

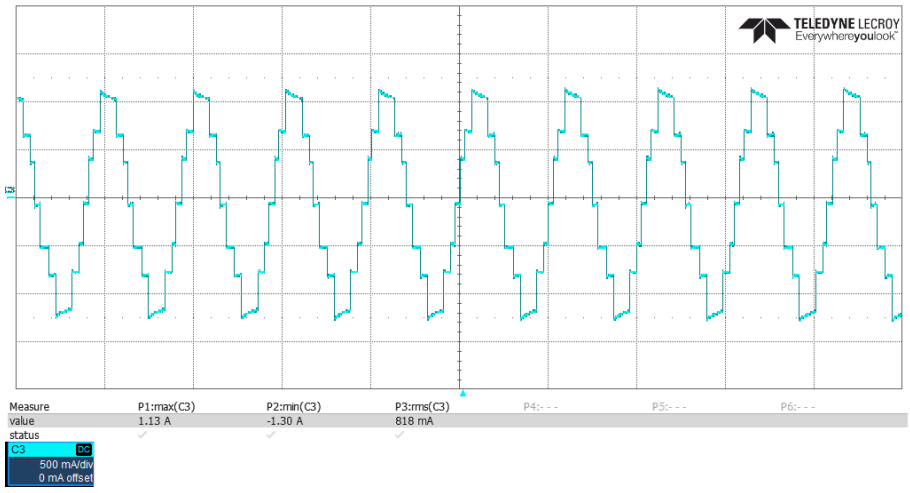

(c)

Fig. 10. The 7-level symmetrical CMLI of (a) the output voltage waveform, (b) the output voltage THD, (c) the output current, when 24 V input voltage of converter is injected

Similarly, when three input voltage of 24 V setup up to 110 V by converter are connected in series (n = 3), the results as shown in Figure 10. Three H-bridge cells were used in the experiment for 7-level CMLI. Each H-bridge was attached to equal 110V dc voltage sources. Figure 10 summarizes the project's findings. Figure 10(a) shows the inverter output voltage waveform. With the 5^{th} and 7^{th} harmonic orders removed, the inverter output voltage THD created from the 7-level CMLI sample was 14.9%, as shown in Figure 10(b). It shows that The harmonic order elimination is better than when input voltage of converter at 18V. The Figure 10(c) of this plot shows the current values for this configuration and the RMS current is 0.82 A_{rms}. Therefore, the total power provide to the infrared load by CMLI system is 187 W.

Figure 10 (a) show the total output voltage levels for a 7 level CMLI and Figure 11 (a), (b), (c) shows the individual output voltages across each of the bridge. As shown in Figures 10(a) the total output voltage of a multilevel inverter is the summation voltages found across all the output bridges in Figure 11 (a), (b), (c).

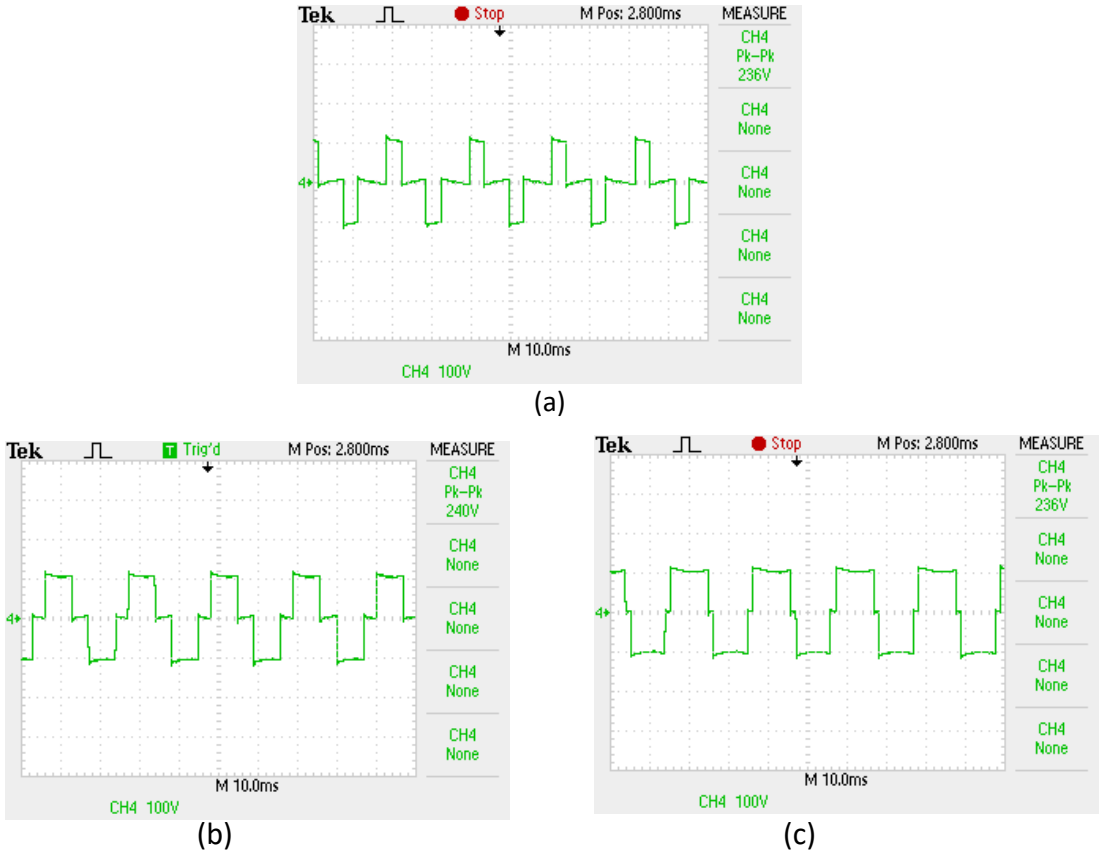

Fig. 11. Individual bridge voltage for 7 level CMLI when the input voltage of converter is 24 V

As illustrated in Figure 11, the values measured is the input current injected to the boost converter. Then, the converters step up 24 V to 110 V output voltage are connected to each H-bridge of CMLI. The voltage level of each bridge linked to the converter was shown in Figure 12. It can be seen that all three converters required around 5~8 A to achieve a 110 V step up.

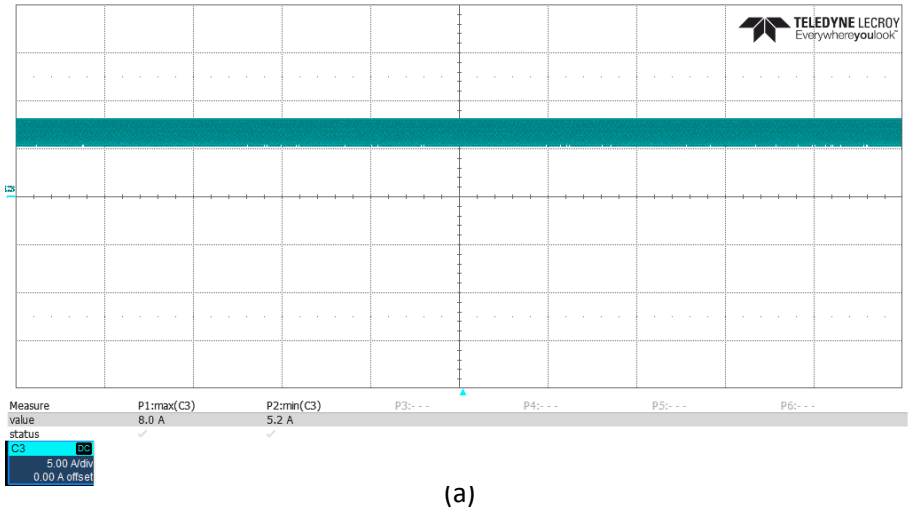

(a)

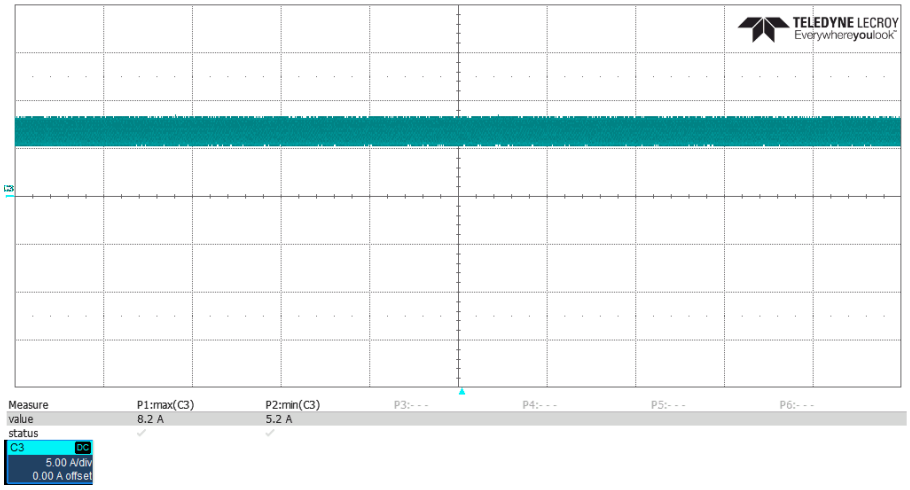

(b)

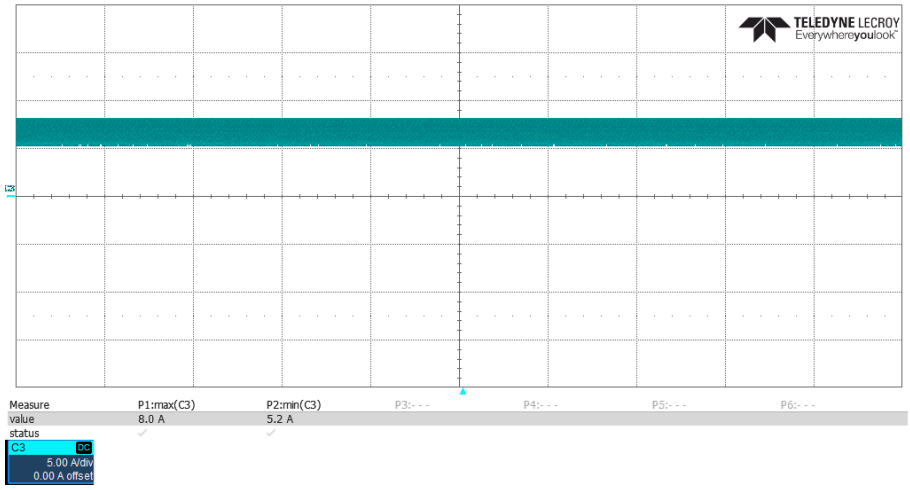

(c)

Fig. 12. Input current consumed of all three converters when step up voltage from 24 V to 110 V

4.Conclusions

The complete two stage inverter is now accomplish tested at prototype level. In this CMLI scheme each of the boost converter and the inverter module communicate with each other via the network signals and the microcontrollers. It is observed that the output voltage across each of the individual bridge equals the total system output voltage. These THD produced is not the lowest that is produced in an inverter system. Based on another sources of research have stated that there is a method to successfully reduce 17.71% of THD by compensating the dead time (DT). To fix the distortion caused by the DTs, a number of corrective techniques have been put forth. In order to maintain the optimum area, the suggested DT compensator adds a compensatory pulse at the end of each pulse in order to compensate for its area without changing the original pulse width [17].

The simulation results shown the differences between 18V and 24V of voltage supply in term duty cycle of PWM, current consumption, and output voltage from the circuit. The circuit is tested, and the output findings are compared to the concept, indicating that it fits the design specifications and current circumstances. Based on the results obtained, it can be assumed that when the disparity between the voltage levels (input vs output) of the boost converter was smaller, the control effort required by this controller becomes considerably more significant.

Acknowledgment
This work is supported by Research Management Centre of Universiti Malaysia Perlis.

References

[1] Sahoo, Sarat Kumar, Sukruedee Sukchai, and Franco Fernando Yanine. "Review and comparative study of single-stage inverters for a PV system." *Renewable and Sustainable Energy Reviews* 91 (2018): 962-986. https://doi.org/10.1016/j.rser.2018.04.063

[2] Azli, N. Ahmad, and H. Jaffar. "Performance Analysis of an Active Power Filter Utilizing Cascaded H-Bridge Multilevel Inverter with Unified Constant-frequency Integration Control." *Journal of Advanced Research in Applied Mechanics* 16, no. 1 (2015): 15-22.

[3] Anita, S. Jensie, Y. Shakil Ahmed, D. Haris Prabhu, and S. L. Govind. "Proposed modified solar based dc-dc quadratic boost converter for modern irrigation system." *Materials Today: Proceedings* 33 (2020): 4656-4662. https://doi.org/10.1016/j.matpr.2020.08.306

[4] M. A. Iqbal, "Transformer-Less Inverter," vol. 10, no. 05, pp. 359–360, 2021.

[5] Wang, Lu, Yanjun Shi, Yuxiang Shi, Ren Xie, and Hui Li. "Ground leakage current analysis and suppression in a 60-kW 5-level T-type transformerless SiC PV inverter." *IEEE Transactions on Power Electronics* 33, no. 2 (2017): 1271-1283. https://doi.org/10.1109/TPEL.2017.2679488

[6] Raji, Atanda K., and Mohamed TE Kahn. "Investigation of common-mode voltage and ground leakage current of grid-connected transformerless PV inverter topology." *Journal of Energy in Southern Africa* 26, no. 1 (2015): 20-24. https://doi.org/10.17159/2413-3051/2015/v26i1a2217

[7] Gayen, P. K. "Novel control approach for enhancing multi-performance of two-stage converter during power transfer from solar photo-voltaic array to AC grid." *Sustainable Energy Technologies and Assessments* 45 (2021): 101132. https://doi.org/10.1016/j.seta.2021.101132

[8] Yang, Zhaoxia, Jianwu Zeng, Dianzhi Yu, Qun Zhang, and Zhe Zhang. "Two-stage power decoupling for a single-phase photovoltaic inverter by controlling the DC-link voltage ripple in the dq frame." In *2020 IEEE Applied Power Electronics Conference and Exposition (APEC)*, pp. 424-429. IEEE, 2020. https://doi.org/10.1109/APEC39645.2020.9124473

[9] Zeb, Kamran, Saif Ul Islam, Waqar Ud Din, Imran Khan, Muhammad Ishfaq, Tiago Davi Curi Busarello, Iftikhar Ahmad, and Hee Je Kim. "Design of fuzzy-PI and fuzzy-sliding mode controllers for single-phase two-stages grid-connected transformerless photovoltaic inverter." *Electronics* 8, no. 5 (2019): 520. https://doi.org/10.3390/electronics8050520

[10] Santhoshi, B. Kavya, K. Mohanasundaram, and L. Ashok Kumar. "ANN-based dynamic control and energy

management of inverter and battery in a grid-tied hybrid renewable power system fed through switched Z-source converter." *Electrical Engineering* 103, no. 5 (2021): 2285-2301. https://doi.org/10.1007/s00202-021-01231-7

[11] Ludin Lawrence, Derick Joy, Jeswin Paul, Fathmathul Zuhra, and Sebin Davis. "Design and Evaluation of Voltage Control using Static Stabilizer."

[12] Coelho, Roberto Francisco, Lenon Schimtz, and Denizar Cruz Martins. "Grid-connected PV-wind-fuel cell hybrid system employing a supercapacitor bank as storage device to supply a critical DC load." In *2011 IEEE 33rd international telecommunications energy conference (INTELEC)*, pp. 1-10. IEEE, 2011. https://doi.org/10.1109/INTLEC.2011.6099817

[13] Ghaderi, Davood, Sanjeevikumar Padmanaban, Pandav Kiran Maroti, Behnaz Papari, and Jens Bo Holm-Nielsen. "Design and implementation of an improved sinusoidal controller for a two-phase enhanced impedance source boost inverter." *Computers & Electrical Engineering* 83 (2020): 106575. https://doi.org/10.1016/j.compeleceng.2020.106575

[14] Kumar, GV Brahmendra, Palanisamy Kaliannan, Sanjeevikumar Padmanaban, Jens Bo Holm-Nielsen, and Frede Blaabjerg. "Effective management system for solar PV using real-time data with hybrid energy storage system." *Applied Sciences* 10, no. 3 (2020): 1108. https://doi.org/10.3390/app10031108

[15] Hoon, Yap, Mohd Amran Mohd Radzi, Mohd Khair Hassan, and Nashiren Farzilah Mailah. "DC-link capacitor voltage regulation for three-phase three-level inverter-based shunt active power filter with inverted error deviation control." *Energies* 9, no. 7 (2016): 533. https://doi.org/10.3390/en9070533

[16] Zheng, Sheng, Ze Ni, and Madhu Chinthavali. "A Flexible and Secure Evaluation Platform for Overvoltage Protection in Power Electronics Systems." In *2020 IEEE Transportation Electrification Conference & Expo (ITEC)*, pp. 877-882. IEEE, 2020. https://doi.org/10.1109/ITEC48692.2020.9161571

[17] Oliva, A., H. Chiacchiarini, A. Aymonino, and P. Mandolesi. "Reduction of total harmonic distortion in power inverters." *Latin American applied research* 35, no. 2 (2005): 89-93.